# Supporting Infoirmation

## Energy harvesting from $NiCo_2S_4/Co_xS_y$ nanoflakes: Two-fold strategy by morphology control & redox additive electrolyte

Love Bansal[1], Deb Kumar Rath[1], Shivansh Raj Pandey[1],Bhumika Sahu[1], Nikita Ahlawat[1], Subin Kaladi Chondath[1*], Rajesh Kumar[1,2*].

[1]Material and Devices Laboratory, Department of Physics, Indian Institute of Technology Indore, Simrol-453552, India

[2] Centre for Advanced Electronics, Indian Institute of Technology Indore, Simrol-453552, India

*Email: rajeshkumar@iiti.ac.in (RK); subinkc@iiti.ac.in (SKC)

## S1: Characterization details

A Horiba Jobin–Yvon Raman spectrometer with a 633 nm excitation laser was used to record the Raman spectrum of all the electrodes. A Rigaku X-ray diffractometer (Cu $K_{\alpha}$ radiation of 1.54 Å wavelength) was used for X-ray diffraction (XRD) of all the electrodes. A Supra 55 Zeiss scanning electron microscopy (SEM) was used for surface morphology and elemental distribution X-ray (EDX) mapping of all the electrodes. Instrument: X-ray photoelectron spectroscopy (XPS, PHI 5000 VersaProbe II, ULVAC-PHI Inc., USA) equipped with micro-focused (100 μm, 15 kV) monochromatic Al-Kα X-Ray source (hν = 1486.6 eV). Both survey spectra and narrow scans (high-resolution spectra) were recorded. Survey scans were recorded with an X-ray source power of 50W and pass energy of 187.85 eV. High-resolution spectra of the major elements were recorded at 46.95 eV pass energy. XPS data were processed using PHI's Multipak software. The binding energy was referenced to the C 1s peak at 284.8 eV.. A Metrohm-Multi Autolab M204 potentiostat was used for deposition and the device's electrochemical measurements.

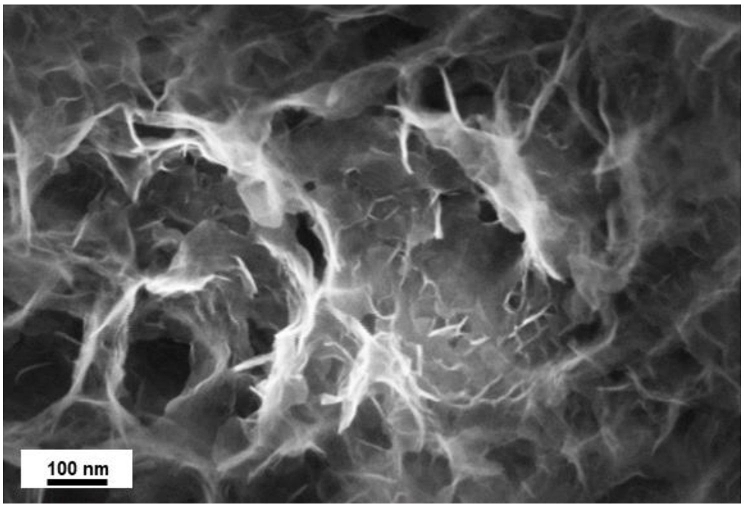


Figure S1: High magnification SEM image of NCS/CS.

Table S1: Chemical composition of the NCS/CS complex over CC.

| S.No | Atom | Percentage Contribution (%) |
|---|---|---|
| 1 | Ni | 8.35 |
| 2 | Co | 26.51 |
| 3 | S | 45.83 |

## S2: Electrochemical measurements of electrode

The electrochemical properties of electrodes were investigated using the conventional three-electrode system, with electroactive material $NiCo_2S_4/Co_xS_y$ (NCS/CS) as the working electrode, Pt wire as a counter electrode, and Ag/AgCl as a reference electrode in 1 M KOH with or without 0.05 M $K_3[Fe(CN)_6]$ in 20 ml DI as electrolyte. The cyclic voltammetry (CV) curves were obtained at several scan rates (5 to 50 mV/s), within a wide potential range of -0.1 V to 0.7 V. The electrochemical impedance spectroscopy of electrodes was done within the frequency range of 10 kHz to 10 mHz at 0.4 V. Galvanostatic charge-discharge (GCD) cycles were obtained at various current densities (1.0 A/g to 10 A/g) within the wide potential window of -0.1 V to 0.45 V.

The specific capacitance of the electrode is calculated in GCD plots using the equation[S1] as below-

$$C_s = \frac{I\Delta t_d}{A\Delta V}\ (F/cm^2), \text{ or } C_s = \frac{I\Delta t_d}{m\Delta V}\ (F/g), \tag{S1}$$

where $\Delta t_d$ is the discharging time, $\Delta V$ is the potential window of the GCD plot, and *I/A* or I/m is the current density of electrode materials on CC (A is the active area of electrode:1.5 $cm^2$ in this case, and m is the mass of active material: 1.5 mg in this case.).

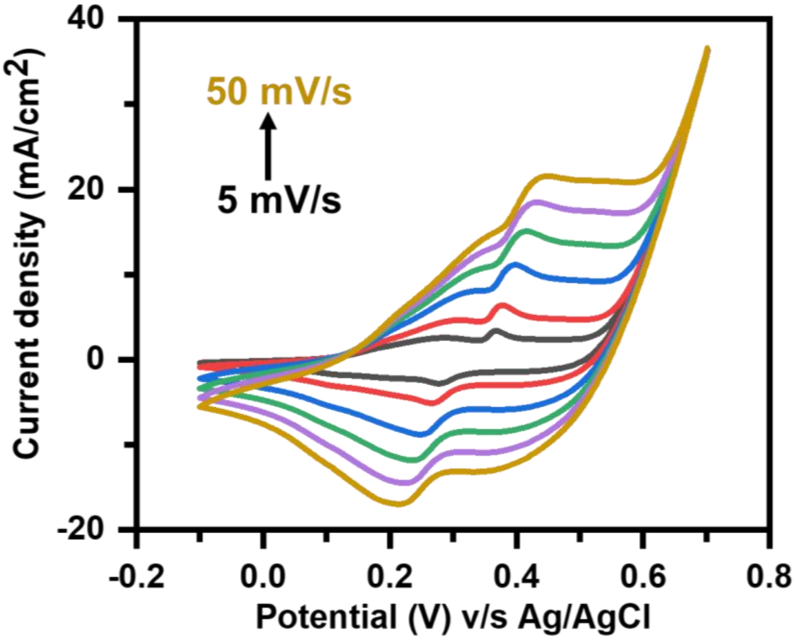


Figure S2: CV cure of NiCo2S4/CoxSy in 1 M KOH at various scan rates.

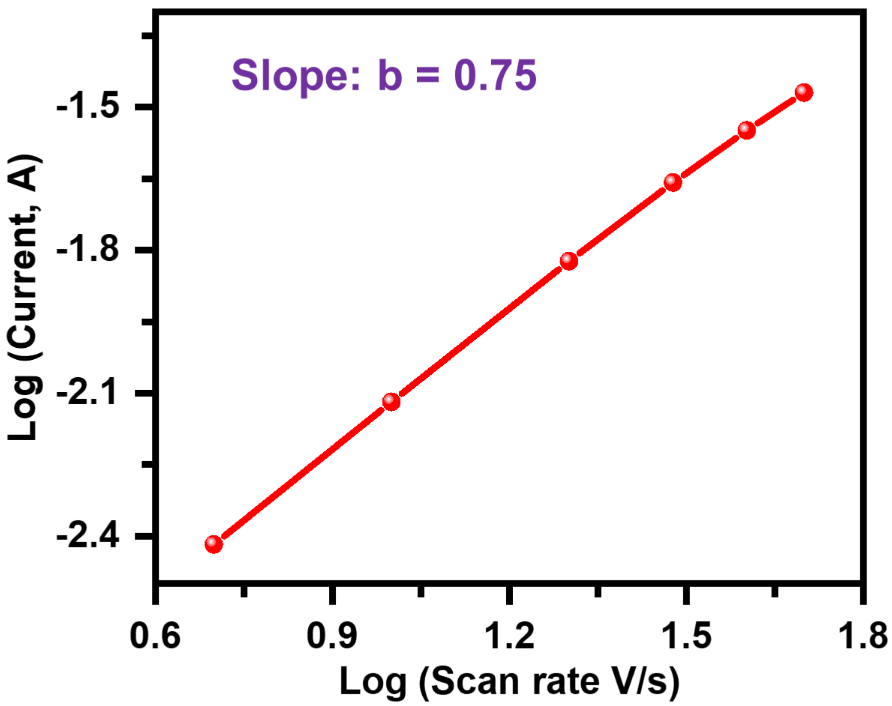


Figure S3: Variation of logarithmic peak current as a function of logarithmic scan rate for NCS/CS electrode in 1 KOH electrolyte.

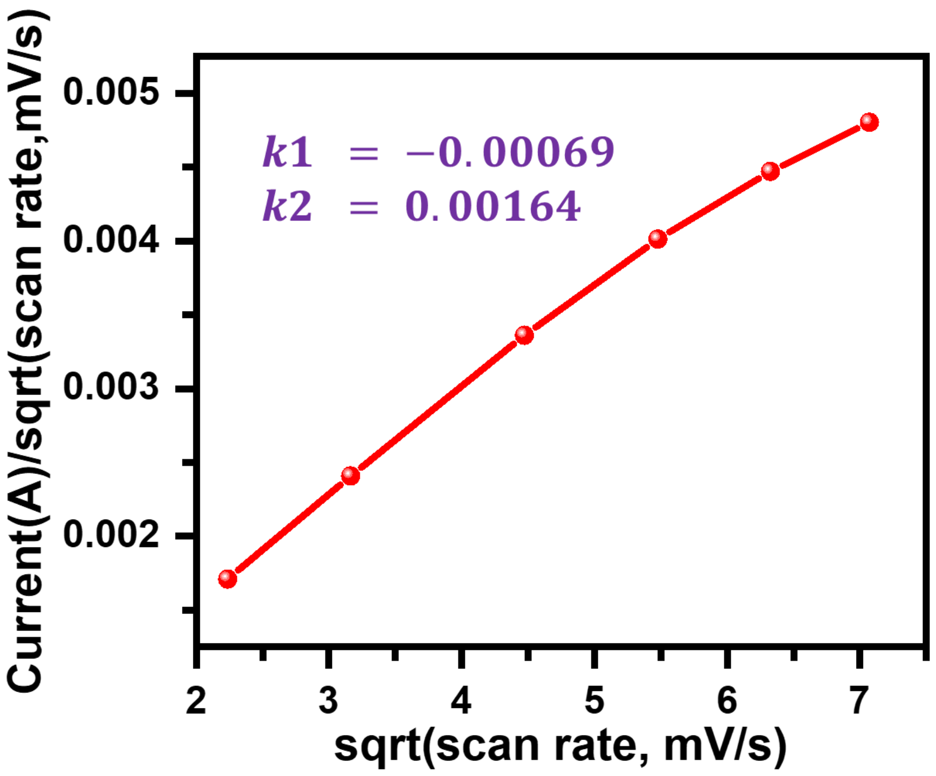


Figure S4: Variation of current/sqrt(scan rate) as a function of sqrt(scan rate) for NCS/CS electrode in 1 KOH electrolyte.

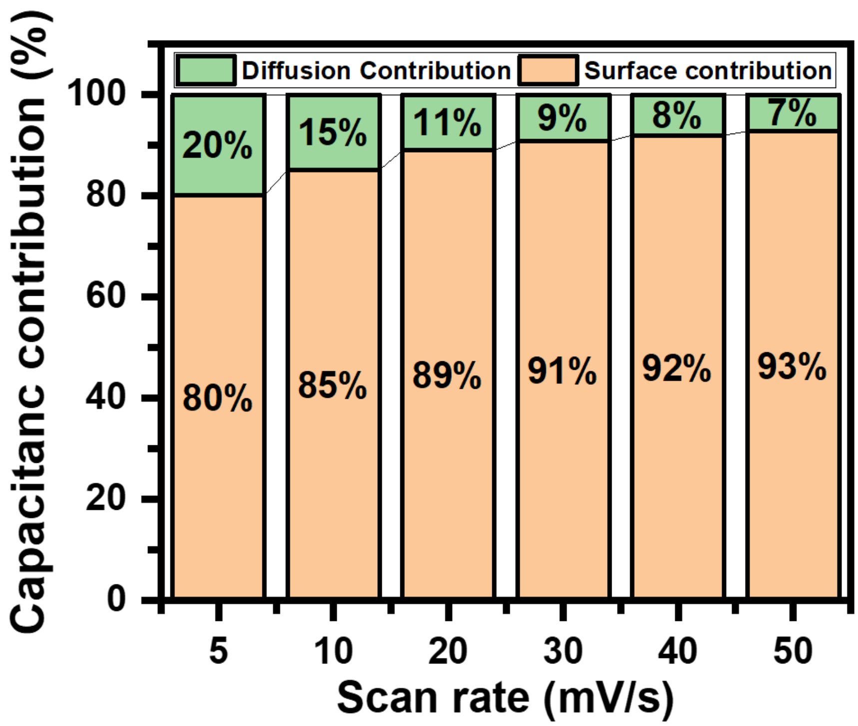


Figure S5: Capacitance contribution graph of NCS/CS electrodes in 1 KOH electrolyte.

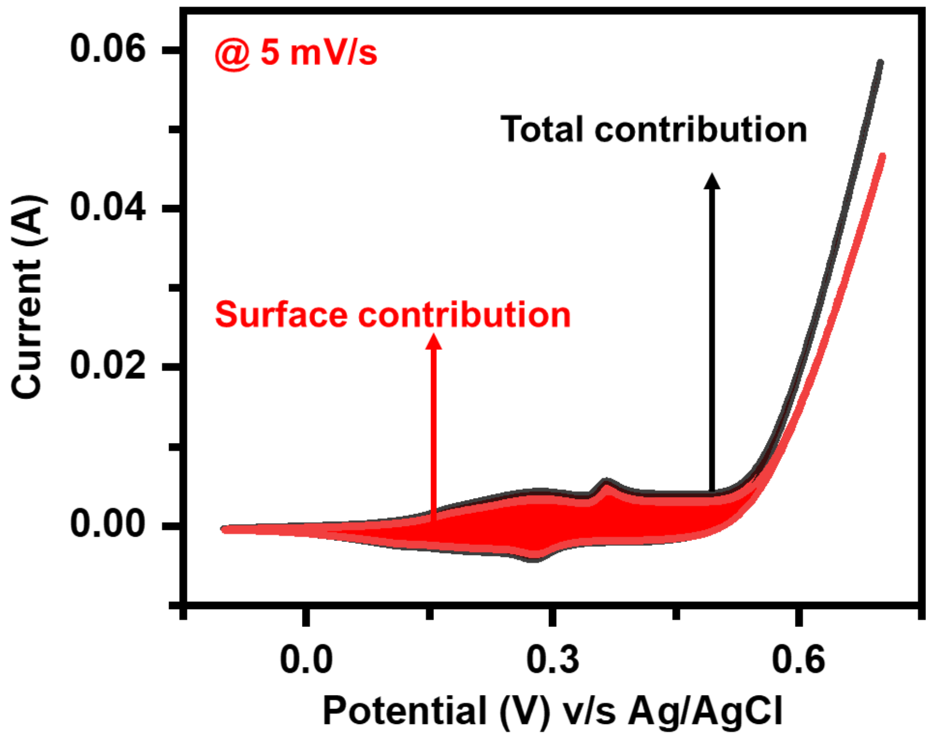


Figure S6: Pictorial representation of dominance of surface-controlled contribution for NCS/CS in 1 M KOH electrolyte at 5 mV/s.

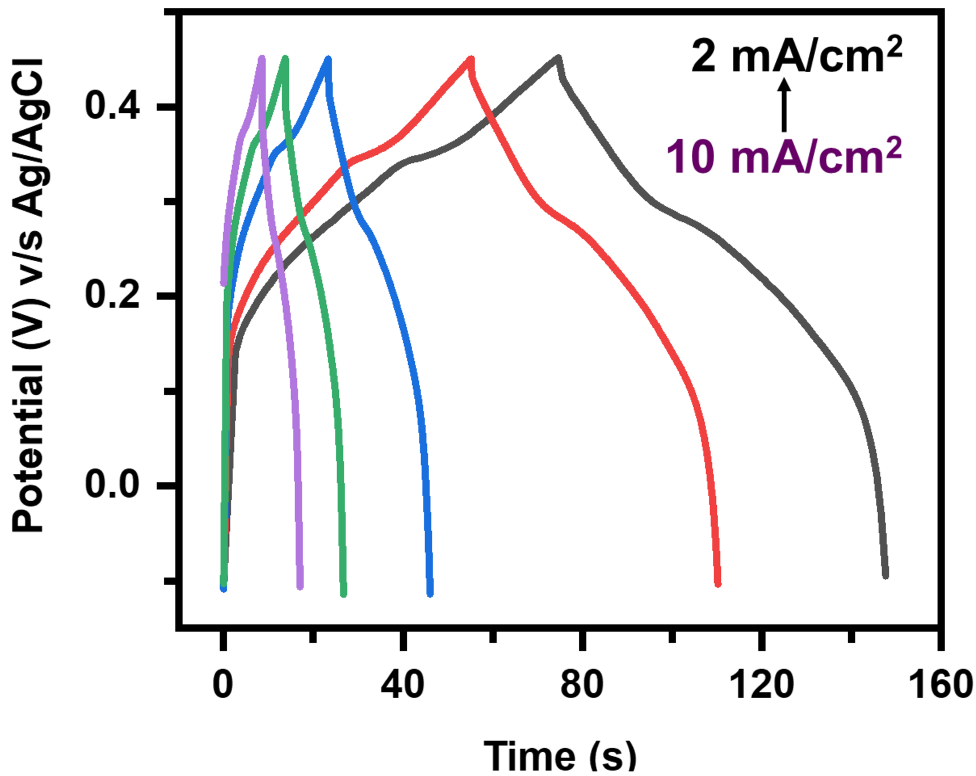

Figure S7: GCD plot of NNCS/CS electrodes in 1 M KOH electrolyte at various current densities.

Table S2: Specific capacitance comparison table for $NiCo_2S_4$/CS electrode and their composites with already reported literature.

| S.No | Material | Specific capacitance | Current Density | Reference |
|---|---|---|---|---|
| 1 | graphene oxide-$NiCo_2S_4$ | 1640 F/g | 1A/g | Panicker et al.[1] |
| 2 | $NiCo_2S_4$@$NiMoO_4$/NF | 2006 F $g^{-1}$ | 5 mA $cm^{-2}$ | Zhang et al.[2] |
| 3 | $NiCo_2S_4$ nano-petals | 2036.5 F $g^{-1}$ | 1 A $g^{-1}$ | Wen et al.[3] |
| 4 | $NiCo_2S_4$ urchin balls | 1352.2 F $g^{-1}$ | 1 A $g^{-1}$ | Tian et al.[4] |
| 5 | FCP@ $NiCo_2S_4$ | 3115 mF $cm^{-2}$ | 2 mA $cm^{-2}$ | Wu et al.[5] |
| 6 | $NiCo_2S_4$@PPy | 1524 F $g^{-1}$ | 4 mA $cm^{-1}$ | Meng et al.[6] |
| 7 | V/MWCNTs | 2080 F $g^{-1}$ | 1 A $g^{-1}$ | Sajjad et al.[7] |
| 8 | $NiCo_2S_4$/CNT | 2210 F $g^{-1}$ at 1 A g | 1 A $g^{-1}$ | Lu et al.[8] |
| 9 | CC/ $NiCo_2S_4$@Zn–Ni–Co–S | 2668 F $g^{-1}$ | 1 A $g^{-1}$ | Peng et al.[9] |
| 10 | $NiCo_2S_4$@rGO | 2418 F $g^{-1}$ | 1A $g^{-1}$ | Zhao et al.[10] |
| 11 | $NiCo_2S_4$@2D-Carbyne nanohybrid | 2507 F $g^{-1}$ | 1 A $g^{-1}$ | Dhandapani et al.[11] |

| | | | | |
|---|---|---|---|---|
| **12** | $NiCo_2S_4$/$\mathbf{Co_xS_y}$ | **7218 F/g** | **2 A/g** | **This work.** |

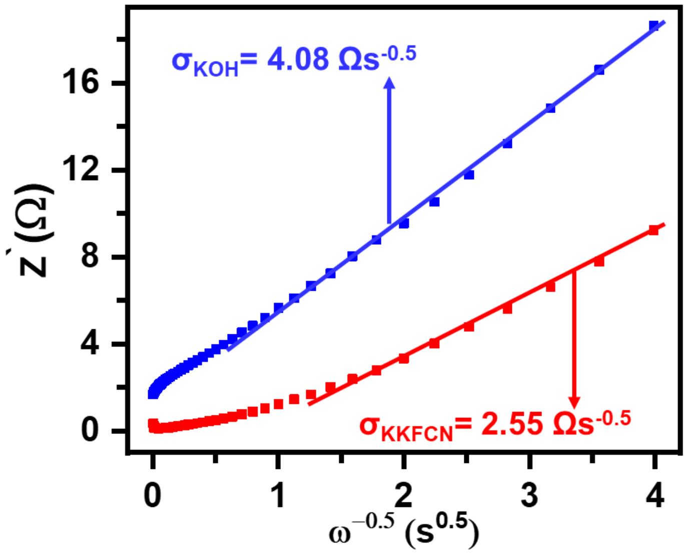


Figure S8: The Warburg factor σ with or without redox additive electrolyte for NCS/CS electrode.

## S3: Specific capacitance, power density, and energy density calculations of solid-state supercapacitor device.

The specific capacitance of a solid-state symmetric supercapacitor device is calculated using equation S2,

$$C_s = \frac{I\Delta t_d}{m\Delta V}\ (F/g), \tag{S2}$$

where *I/m* is the current density of the device. Additionally, the energy density and power density of the device were also calculated at different current densities using the following equation[S3, S4]

$$E = \frac{1}{2} C_s (\Delta V)^2\ (Wh/Kg)\ , \tag{S3}$$

$$P = 3600 \frac{E}{\Delta t_d}\ (W/Kg), \tag{S4}$$

Table S3: Comparison table NCS/CS symmetric supercapacitor device with other previously reported devices.

| S.No | Composition | Capacitance | Current density | Reference |
|---|---|---|---|---|
| 1 | $NiCo_2S_4$/20rGO//AC | 92 F/g | 5 A/g | Zhao et al.[12] |
| 2 | $NiCo_2S_4$/PANI//AC | 130 F/g | 4 A/g | He et al.[13] |
| 3 | $NiCo_2S_4$@PANI/CF//graphene/CF | 182 F/g | 5 A/g | Liu et al.[14] |
| 4 | $NiCo_2S_4$/Co9S8 HSs//AC | 196 F/g | 5 A/g | Han et al.[15] |
| 5 | P doped Co–Ni–S//AC | 155.4 F/g | 5 A/g | Meng et al.[16] |
| 6 | $NiCo_2S_4$@NiCo2S4//AC | 83 F/g | 4 A/g | Rong et al.[17] |
| 7 | $NiCo_2S_4$@GR//AC | 120 F/g | 4 A/g | Xiao et al.[18] |
| 8 | PNTs@ $NiCo_2S_4$//PNTs@ $NiCo_2S_4$ | 165 F/g | 5 A/g | Zhang et al.[19] |
| 9 | $NiCo_2S_4$@PPy//AC | 1.528 $mAh/cm^2$ | 5 $mA/cm^2$ | Chen et al.[20] |
| **10** | $NiCo_2S_4$/$\mathbf{Co_xS_y}$ | **380 F/g** | **1 A/g** | **This work** |

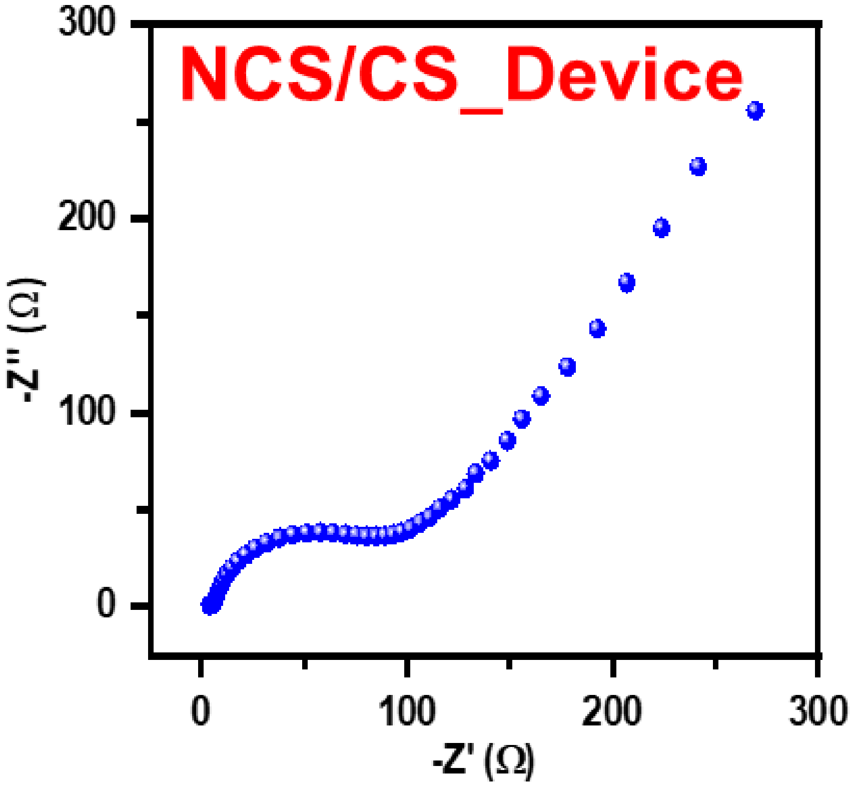


Figure S9: EIS spectra of NCS/CS symmetric supercapacitor device.

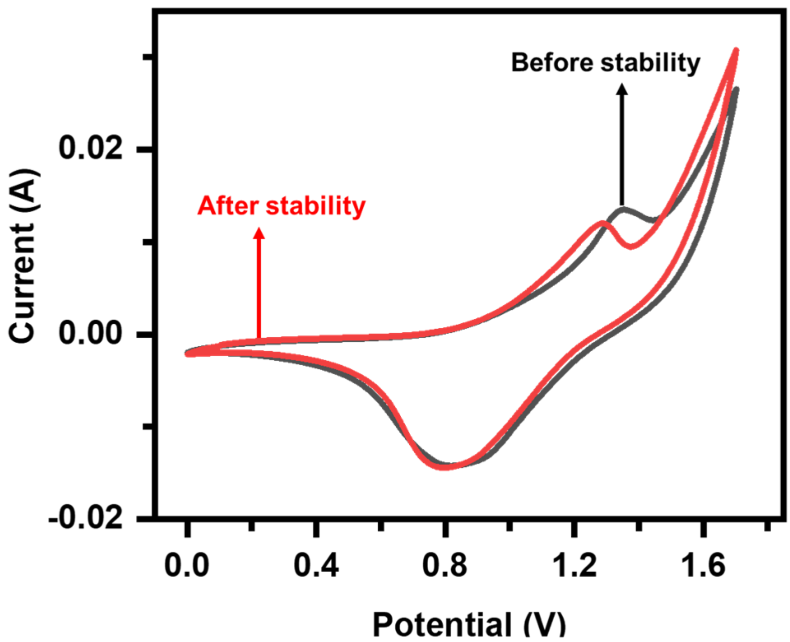


Figure S10: CV curve of the device before and after stability measurements.

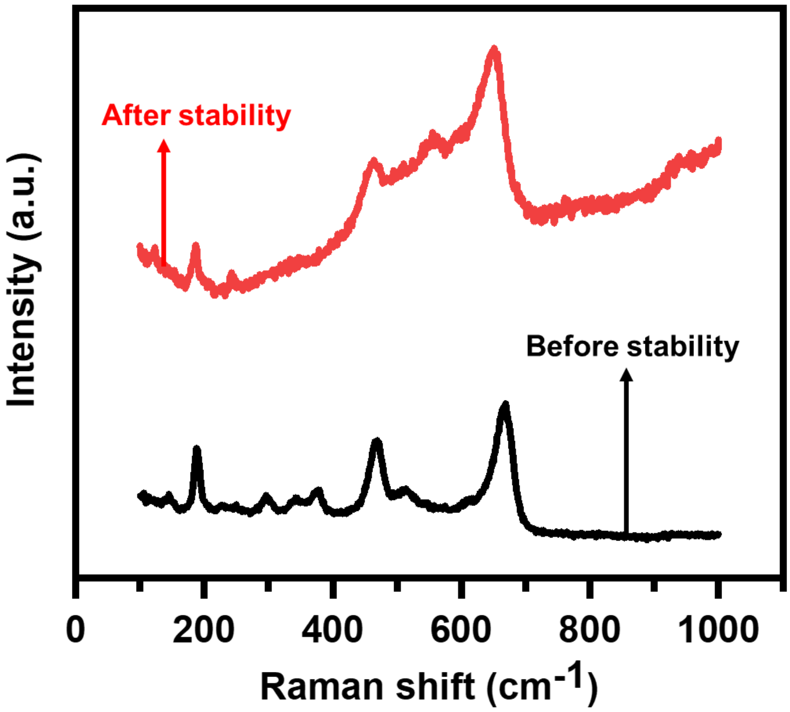


Figure S11: Raman Spectrum of the NCS/CS device before and after stability measurements.

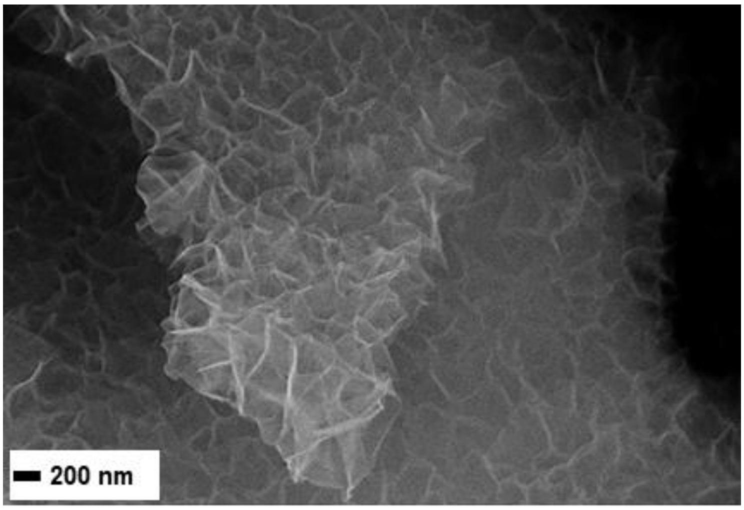


Figure S12: SEM image of NCS/CS complex after stability measurements.

## References


1 N. J. Panicker and P. P. Sahu, *Diamond and Related Materials*, 2023, **136**, 109936.
2 Y. Zhang, J. Xu, Y. Zheng, Y. Zhang, X. Hu and T. Xu, *Nanoscale Res Lett*, 2017, **12**, 412.
3 Y. Wen, S. Peng, Z. Wang, J. Hao, T. Qin, S. Lu, J. Zhang, D. He, X. Fan and G. Cao, *J. Mater. Chem. A*, 2017, **5**, 7144–7152.
4 J. Tian, J. Zhang and X. Li, *RSC Adv.*, 2024, **14**, 9587–9593.

5 H. Wu, J. Bi, Y. Li, L. Wang, X. Pang, C. Xiong and Z. Li, *Journal of Materiomics*, 2021, **7**, 166–176.
6 F. Y. Meng, Y. F. Yuan, S. Y. Guo and Y. X. Xu, *Materials Technology*, 2017, **32**, 815–822.
7 M. Sajjad, X. Chen, C. Yu, L. Guan, S. Zhang, Y. Ren, X. Zhou and Z. Liu, *J. Mol. Eng. Mater.*, 2019, **07**, 1950004.
8 Y. Lu, Z. Zhang, X. Liu, W. Wang, T. Peng, P. Guo, H. Sun, H. Yan and Y. Luo, *CrystEngComm*, 2016, **18**, 7696–7706.
9 Z. Peng, L. Gong, J. Huang, Y. Wang, L. Tan and Y. Chen, *Carbon*, 2019, **153**, 531–538.
10 Y. Zhao, H. Zhang, Y. Lin, J. Chen, K. Li and A. Cheng, *Diamond and Related Materials*, 2020, **108**, 107925.
11 P. Dhandapani, A. K. Subbiah Petchimuthuraju, S. Prasad Rajendra, M. S. AlSalhi and S. Angaiah, *ChemPhysChem*, 2024, **25**, e202300658.
12 J. Zhao, Z. Wei, C. Wang, M. Zhou and C. Lu, *Ionics*, 2024, **30**, 1723–1733.
13 X. He, Q. Liu, J. Liu, R. Li, H. Zhang, R. Chen and J. Wang, *Chemical Engineering Journal*, 2017, **325**, 134–143.
14 X. Liu, Z. Wu and Y. Yin, *Chemical Engineering Journal*, 2017, **323**, 330–339.
15 X. Han, Q. Chen, H. Zhang, Y. Ni and L. Zhang, *Chemical Engineering Journal*, 2019, **368**, 513–524.
16 Y. Meng, P. Sun, W. He, B. Teng and X. Xu, *Nanoscale*, 2019, **11**, 688–697.
17 H. Rong, T. Chen, R. Shi, Y. Zhang and Z. Wang, *ACS Omega*, 2018, **3**, 5634–5642.
18 Y. Xiao, D. Su, X. Wang, L. Zhou, S. Wu, F. Li and S. Fang, *Electrochimica Acta*, 2015, **176**, 44–50.
19 J. Zhang, H. Guan, Y. Liu, Y. Zhao and B. Zhang, *Electrochimica Acta*, 2017, **258**, 182–191.
20 S. Chen, Y. Yang, Z. Zhan, J. Xie and J. Xiong, *RSC Advances*, 2017, **7**, 18447–18455.